Original Article

Urinary gas chromatography mass spectrometry metabolomics in asphyxiated newborns undergoing hypothermia: from the birth to the first month of life

Antonio Noto[1], Giulia Pomero[2], Michele Mussap[3], Luigi Barberini[4], Claudia Fattuoni[5], Francesco Palmas[5], Cristina Dalmazzo[2], Antonio Delogu[2], Angelica Dessì[1], Vassilios Fanos[1], Paolo Gancia[2]

[1]Department of Surgical Sciences, University of Cagliari and Neonatal Intensive Care Unit, Puericulture Institute and Neonatal Section, Azienda Ospedaliera Universitaria, Cagliari, Italy; [2]Neonatal Intensive Care, Neonatology, ASO S. Croce e Carle, Cuneo, Italy; [3]Laboratory Medicine Service, IRCCS AOU San Martino-IST, University-Hospital, Genoa, Italy; [4]Department of Medical Sciences and Public Health, [5]Department of Chemical and Geological Sciences, University of Cagliari, Cagliari, Italy

Contributions: (I) Conception and design: A Dessì, V Fanos, P Gancia; (II) Administrative support: None; (III) Provision of study materials or patients: G Pomero, C Dalmazzo, A Delogu, V Fanos, P Gancia; (IV) Collection and assembly of data: A Noto, L Barberini, C Fattuoni, F Palmas, A Dessì; (V) Data analysis and interpretation: A Noto, L Barberini, C Fattuoni, F Palmas; (VI) Manuscript writing: All authors; (VII) Final approval of manuscript: All authors.

Correspondence to: Michele Mussap, MD. Laboratory Medicine Service, IRCCS AOU San Martino-IST, University-Hospital, National Institute for Cancer Research, Largo Rosanna Benzi, 10 Genova (16132), Italy. Email: michele.mussap@hsanmartino.it.

Background: Perinatal asphyxia is a severe clinical condition affecting around four million newborns worldwide. It consists of an impaired gas exchange leading to three biochemical components: hypoxemia, hypercapnia and metabolic acidosis.

Methods: The aim of this longitudinal experimental study was to identify the urine metabolome of newborns with perinatal asphyxia and to follow changes in urine metabolic profile over time. Twelve babies with perinatal asphyxia were included in this study; three babies died on the eighth day of life. Total-body cooling for 72 hours was carried out in all the newborns. Urine samples were collected in each baby at birth, after 48 hours during hypothermia, after the end of the therapeutic treatment (72 hours), after 1 week of life, and finally after 1 month of life. Urine metabolome at birth was considered the reference against which to compare metabolic profiles in subsequent samples. Quantitative metabolic profiling in urine samples was measured by gas chromatography mass spectrometry (GC-MS). The statistical approach was conducted by using the multivariate analysis by means of principal component analysis (PCA) and orthogonal partial least square discriminant analysis (OPLS-DA). Pathway analysis was also performed.

Results: The most important metabolites depicting each time collection point were identified and compared each other. At birth before starting therapeutic hypothermia (TH), urine metabolic profiles of the three babies died after 7 days of life were closely comparable each other and significantly different from those in survivors.

Conclusions: In conclusion, a plethora of data have been extracted by comparing the urine metabolome at birth with those observed at each time point collection. The modifications over time in metabolites composition and concentration, mainly originated from the depletion of cellular energy and homeostasis, seems to constitute a fingerprint of perinatal asphyxia.

Keywords: Metabolomics; perinatal asphyxia; hypoxic-ischemic-encephalopathy; newborns; metabolites; biomarkers; urine

Submitted Sep 25, 2016. Accepted for publication Oct 25, 2016.
doi: 10.21037/atm.2016.11.27
View this article at: http://dx.doi.org/10.21037/atm.2016.11.27

Introduction

Perinatal asphyxia was previously defined as severe lack of oxygen and perfusion to the fetus, especially in the fetal brain, around the time of birth (1). Over the last decades, terms as perinatal asphyxia, birth asphyxia, fetal distress, hypoxic-ischemic encephalopathy (HIE) have been replaced with an "umbrella term": neonatal death associated with acute intrapartum events (2). This change was promoted by several consensus statements on the basis of a paradigm shift in the epidemiologic measurement of intrapartum injury: from process-based or symptom-based indicators to outcome-based measures of mortality and acute morbidity. Unfortunately, the "umbrella term" is long and not user-friendly and thus conventional terms are yet widely used in the literature and in clinical practice. Perinatal asphyxia can be fatal; it is yet one of the primary causes of early neonatal mortality worldwide, affecting 4 million babies per year and causing the death of around 1 million subjects (3). In survivors, brain injuries due to HIE lead to severe disability (4); indeed, the lack of oxygen involves primarily brain, heart, kidney, lung, and gut causing organ injuries and permanent damages (5). The timing of the organ insult is a key factor influencing the extension and the pattern of the damage and, in turn the clinical outcome. The brain is the most injured organ by perinatal asphyxia (6); almost all of the oxygen consumed by the human brain is utilized for the oxidation of glucose, which in turn is the only significant substrate for energy in cerebral metabolism. In detail, the aerobic glycolysis generates pyruvate; subsequently, pyruvate enters into the citric acid cycle, also known as the tricarboxylic acid (TCA) cycle or the Krebs cycle, within mitochondria, ultimately generating adenosine triphosphate (ATP). Neonatal hypoxic/ischemic events remarkably modify these biochemical pathways, leading to energy failure due to: shift from aerobic to anaerobic metabolism; mitochondrial injury with a reduced ATP production; lactate accumulation; over-production of reactive oxygen species (ROS); decreased protein phosphorylation (7,8). As a result, all the energy-dependent mechanisms reduce their activities, leading to neuronal depolarization, cell swelling, and loss of cell homeostasis (9). Depending on various factors, such as the severity of injury and the early retrieval of cerebral blood flow, several neurons may recover their functions by reversing the chemical gradient and restoring the integrity of the membrane. Conversely, other neurons lose completely their functions and interconnections. Current evidences suggest that perinatal asphyxia can alter gene expression, inducing epigenetic changes in DNA methylation, histone modifications and modifying the rate of noncoding RNA synthesis (10); in addition, the response to asphyxia depends on genetic and epigenetic key factors, integrated each other (11,12). Therapeutic hypothermia (TH), a brain cooling technique, usually maintained over 72 hours after the hypoxic-ischemic event, has gained consensus for the treatment of perinatal asphyxia and HIE, reducing the mortality rate and long-term neurodevelopmental disabilities at 12–24 months of age (13,14). TH induces a slowdown in cerebral metabolism of approximately 5% every one degree fall in temperature, delaying the onset of anoxic cell depolarization (15). Unfortunately, despite TH treatment several children continue either to die or to suffer moderate-severe handicaps. Therefore, there is the need to investigate changes in molecular pathways during perinatal asphyxia and TH; the holistic approach offers two advantages over existing methods: comprehensiveness and complementarity (16). Metabolomics, one of the youngest 'omics' disciplines, encompasses comprehensive metabolites evaluation, pattern recognition, and statistical analysis, with the intent to identify and quantify metabolites related with a physiological or a pathological process (17,18). Emerging studies on animal model have highlighted the importance to recognize the metabolic fingerprint in perinatal anoxia-hypoxia (19-21). In newborns with perinatal asphyxia, a small number of metabolomics studies have been published in the literature (22-27); each of them has depicted the metabolic snapshot of the disease. As recapitulated in a recent review (28), human metabolomics studies have found that the most impaired molecular pathway during perinatal asphyxia and TH are the TCA cycle and the osmoregulation system.

The aim of this longitudinal experimental study was to identify the urine metabolome of newborns with perinatal asphyxia at birth (Time 0, T0), corresponding to the admission to the neonatal intensive care unit (NICU) and then to follow changes in urine metabolic profile over time: at 48 hours, during the TH (T1); at the end of the TH (T2, corresponding to 72 hours); after 1 week (T3); after 1 month (T4). The experimental design has been plotted in *Figure 1*.

Methods

Patients population

We included 12 newborns (11 full-terms and one preterm) with perinatal asphyxia, admitted in the NICU of S. Croce

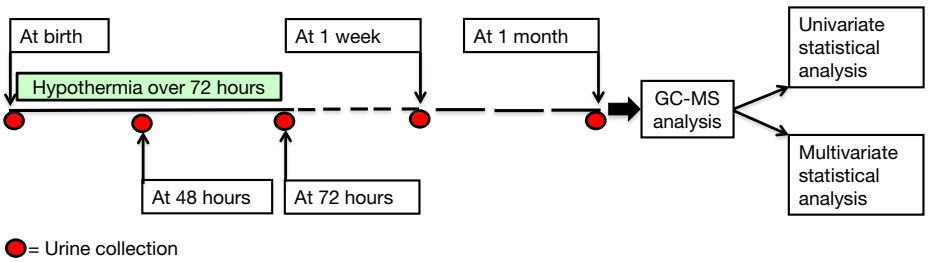

Figure 1 Plot of the experimental design. Red dots indicate the urine collection points.

e Carle hospital, Cuneo, Italy. Their main demographic and clinical characteristics are summarized in *Table 1*. The study was approved by institutional ethics board of Cagliari (CA-206-18/03/2013); parents gave written informed consent to the study. Asphyxia diagnosis was performed by using the Sarnat grading scale (Sarnat staging), based on the infant's clinical findings and neurologic signs (29). All the babies were treated with hypothermia over 72 hours; urine samples were collected at different time points. The time sequence of samples collection was: at birth, when they were admitted to the NICU (T0); after 48 hours (T1); after 72 hours (T2); after 1 week (T3); after 1 month (T4). Neurodevelopmental outcome was evaluated later, at one year of age by using the Bayley Scales of Infant and Toddler Development (cognitive, language, motor function, social-emotional, adaptive behaviour scale)—3rd Edition (Bayley-III) (30).

Samples collection, storage and preparation

The overall number of urine samples collected from 12 newborns over the first month of life was 43; such samples were not available (dead babies), while others were insufficient for analysis or missed (vial breakage during transport or centrifugation), as detailed in *Table 2*. Each urine sample (volume around 2–3 mL) was collected by a non-invasive method: a ball of cotton was inserted into the disposable diaper; then urine was aspired with a syringe and transferred to a sterile 2 mL vial. After collection, all the vials were centrifuged and supernatants were immediately frozen and stored at –80 ℃ until analysis. Sample preparation before analysis consisted of a multi-step procedure. Firstly, urine samples were thawed at room temperature and homogenized by using a vortexer for 5–10 seconds. Secondly, 150 µL were transferred into a tube, where 800 µL of urease solution (1 mg/mL) were added. The resulting solution was sonicated for 30 minutes; at the end of the process, 800 µL methanol were further added. After sample centrifugation, 1,200 µL of supernatant were transferred into a glass vial and dried in a vacuum centrifuge overnight. Subsequently, 30 µL of a 0.24 M solution of methoxylamine hydrochloride in pyridine were added to each vial; samples were further mixed by vortexer and kept at room temperature over 17 hours. Finally, 30 µL of *N*-methyl-*N*-trimethylsilyltrifuoroacetamide (MSTFA) were added, mixed for 1 min by vortexer and kept 1 hour at room temperature. The derivatized samples were diluted with 600 µL of a tetracosane solution (internal standard) in hexane (0.01 mg/mL) just before GC-MS analysis.

Samples analysis and data processing

The derivatized samples were analyzed by using a global unbiased mass spectrometry-based platform with GC-MS incorporating an Agilent 5975C interfaced to the GC 7820 (Agilent Technologies, Palo Alto, CA, USA). The system was equipped with a DB-5ms column (Agilent J&W Scientific, Folsom, CA, USA); the injection temperature was set at 230 ℃ and the detector temperature at 280 ℃. Carrier gas (helium) flow rate was equal to 1 mL/min. GC oven starting temperature program was 90 ℃ with 1 min hold time and ramping at a rate of 10 ℃ per minute, reaching a final temperature of 270 ℃ with 7 min hold time. 1 µL of the derivatized sample was injected in split (1:20) mode. After a solvent delay of 3 min, mass spectra were acquired in full scan mode using 2.28 scans per second, with a mass range of 50–700 Amu. Each acquired chromatogram was analyzed by means of the free software Automated Mass Spectral Deconvolution and Identification System (AMDIS): http://chemdata.nist.gov/mass-spc/amdis. Each peak was identified by comparing the corresponding mass spectra and retention times with those stored in an in-house made library including 255 metabolites. Other metabolites were identified by using the National Institute of Standards and Technology's mass spectral database (NIST08) (31) and

Table 1 Clinical and demographic data of study population

Patient IDEE	Gender (M/F)	Gestational age (w)	Mode of delivery	Apgar score		Birth weight (grams)	Oxygen saturate (%)	Maternal and neonatal clinical characteristics and comorbid conditions
				1 min	5 min			
U001	M	38.7	Induced VD	6	7	2,530	97.8	ICP
U002	F	33.6	Emergency CS	1	4	1,796	91.7	Placental abruption; PPHN
U003	M	41.1	Emergency CS	4	7	3,585	88.3	Fetal bradycardia
U004	M	41.0	Elective VD	MV	MV	3,305	97.7	MOF; death attributable to HIE after 8 days of life
U005	M	40.0	VD + EMV	0	4	4,690	92.4	–
U006	M	38.1	VD + EMV	0	0	3,850	–	Pregnancy-induced hypertension; maternal obesity
U007	M	39.0	Emergency VD	4	7	3,910	79.6	Gestational diabetes
U008	M	36.0	Emergency VD	1	3	3,220	95.4	–
U009	F	41.1	Elective VD	1	1	3,640	97.0	Hypothyroidism related pregnancy with therapeutic treatment
U010	F	39.3	Elective VD	0	0	3,590	97.0	Death attributable to HIE after 6 days of life
U011	F	39.8	VD + EMV	0	4	3,440	87.7	–
U012	F	40.4	Elective VD	0	3	3,950	93.0	Death attributable to HIE after 7 days of life

VD, vaginal delivery; CS, caesarian section; MV, mechanical ventilation; MOF, multi organ failure; EMV, electromagnetic ventouse; HIE, hypoxic-ischemic encephalopathy; ICP, intrahepatic cholestasis of pregnancy; PPHN, persistent pulmonary hypertension.

Table 2 Samples collection map over time

Patient IDEE	U0	U1	U2	U3	U4
001	Y	Y	Y	Y	Y
002	Y	Y	Y	Y	Y
003	Not available	Y	Y	Y	Insufficient
004	Y	Y	Y	Death	Not available
005	Y	Y	Y	Y	Y
006	Y	Y	Y	Insufficient	Missed
007	Y	Y	Missed	Y	Insufficient
008	Y	Y	Y	Insufficient	Not available
009	Y	Y	Missed	Y	Insufficient
010	Y	Y	Y	Death	Not available
011	Y	Y	Y	Missed	Y
012	Y	Y	Y	Death	Not available

U0, U1, U2, U3, U4, urine samples collected at T0 (birth), T1 (48 h after birth), T2 (72 h after birth), T3 (1 week after birth), and T4 (1 month after birth), respectively; Y, available, eligible sample.

the Golm Metabolome Database (GMD) (32). As a result, 122 compounds were accurately identified, whereas 5 additional metabolites were tentatively identified on the basis of GMD data. AMDIS analysis produced a matrix spreadsheet (Microsoft Excel®, Microsoft Co, Redmond, WA, USA) as a preliminary tool for the subsequent chemometric analysis.

Data modeling and statistical analysis

Data were analyzed by applying both the unsupervised and the supervised multivariate statistical approach. Principal component analysis (PCA), the most commonly used unsupervised method (33), was applied to identify specific structures such as clusters, anomalies or trends in a dataset (34,35). Partial least squares-discrimination analysis (PLS-DA) and orthogonal partial least square discriminant analysis (OPLS-DA) were applied as supervised methods to identify important variables with discriminative power (36). OPLS-DA is a data visualization method for the observation of grouping within multivariate data. This supervised analysis employs linear regression, including the class memberships of the samples in the calculation. OPLS is able to rotate the projection, so that the model focuses on the side corresponding to the effect of interest; the result is a clearer group's separation and discrimination. The validity of the OPLS-DA model is assessed by statistical parameters: the correlation coefficient R^2, and the cross-validation correlation coefficient Q^2. PLS-DA and OPLS-DA were computed by using the Soft Independent Modeling of Class Analogy software package (SIMCA, version 13.0, Umetrics, Umea, Sweden) (37). By the supervised analysis we obtained the set of variables importance on partial least squares projections (VIP). The VIP method selects variables by calculating the VIP score for each variable and excluding all the variables with VIP score below 1, a predefined threshold (38). In this study, VIP are those metabolites better characterizing each group. Receiver operating characteristic (ROC) analysis was done for each biomarker, being the method of choice for evaluating biomarker specifications. Ultimately, pathway topology analysis was performed for each of the four time collection points, assuming that the upstream nodes regulated the downstream nodes, and not vice versa. The resulting "metabolome view" depicted all metabolic pathways arranged according to the scores from the enrichment analysis (y-axis) and from topology analysis (x-axis), by using Metaboanalyst 3.0 (39). The goal of pathway analysis was to identify pathways significantly impacting in a given phenotype. Since many pathways were tested simultaneously, P values were adjusted for multiple testing. Concisely, the total value corresponds to the total number of compounds involved in a pathway; the hits value

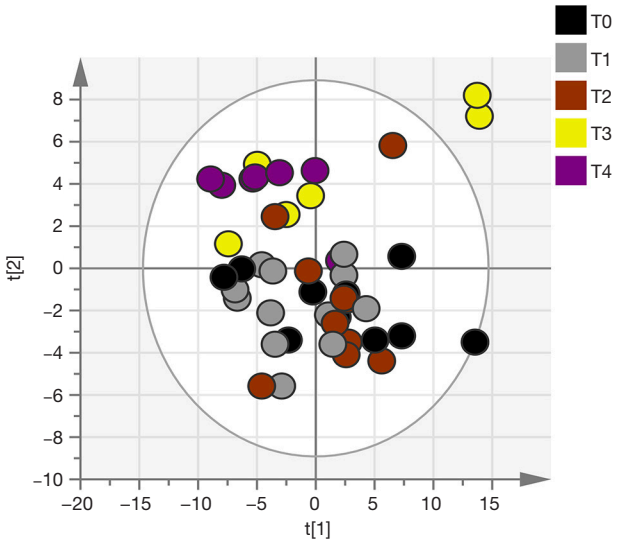

Figure 2 PCA score plot derived from the GC-MS analysis of urine samples in 12 newborns with perinatal asphyxia over the first month of life. T0 = birth (start of TH); T1 =48 hours after birth; T3 =72 hours after birth (end of the TH); T3 =1 week after birth; T4 =1 month after birth. PCA, principal component analysis.

is the actually matched number from the user uploaded data; the raw P value is the original P value calculated by the enrichment analysis; the Holm P value is the P value adjusted by the Holm-Bonferroni method; the impact value represents the metabolic pathway impact calculated from pathway topology analysis (40).

Results

Out of the 12 newborns enrolled in this study, 3 babies (patient IDEE: U004, U010 and U012) died during the 7th day of life. All the deaths were attributable to HIE and comorbid conditions, as reported in *Table 1*. In all of the remaining nine babies, results obtained by using the Bayley III demonstrated the absence of any neurodevelopmental abnormality. The unsupervised PCA was applied to offer a global view on changes over time in urine metabolomics profile. Based on the two principal components (R^2X =0,65; Q^2 =0,36), the resulting plot highlights a "trend in migration" of the metabolic profile for each baby, from T0 to T4 (*Figure 2*); however, the extent of any change and its direction depend on various factors: clinical variables (e.g., prematurity); presence/absence of comorbid conditions (e.g., MODS); clinical outcome (e.g., death). The supervised OPLS-DA model originated a clear separation between metabolic profiles at birth and each of those corresponding to samples collection, as reported in *Figure 3*. Urine metabolome at birth (before starting TH) was considered the reference against which to compare urine metabolome after 48 hours, 72 hours, 1 week and 1 month. Based on the VIP score >1, potential metabolites were identified for each model: after 48 hours, 4 metabolites were found increased and 54 metabolites decreased compared to birth; after 72 hours, 22 were increased and 29 decreased; after 1 week, 24 increased and 19 decreased; after 1 month 5 increased and 33 decreased. To make more significant and comprehensible these results, we reported a partial list of metabolites including those with a continuous trend in changes over time (*Figure 4*). Following this strategy, lactic acid, taurine, lysine, and mannitol decreased systematically from birth; conversely, lactose increased from T1 to T3 when compared with T0, as well as citric acid and galactose from T2 to T4. For each metabolite the area under the curve (AUC) ROC was also calculated. In detail, lactic acid AUC: T1 =0.74, T2 =0.75, T3 =1.0, T4 =0.87. Taurine AUC: T1 =0.66, T2 =0.70, T3 =0.98, T4 =0.91. Lysine AUC: T1 =0.62, T2 =0.65, T3 =0.67, T4 =0.83. Mannitol AUC: T1 =0.65, T2 =0.65, T3 =0.67, T4 =0.87. Lactose AUC: T2 =0.65, T3 =1.0. Citric acid AUC: T2 =0.90, T3 =0.98, T4 =0.97. Other metabolites did not increase or decrease constantly over time. Surprisingly, the unknown metabolite U1710 increased in T1 (AUC =0.82) and T2 (AUC =0.82) and decreased in T3 (AUC =0.80) and in T4 (AUC =0.74), when compared with T0. The most relevant result is the significant difference between the urinary metabolome of the three babies died after 7 days of life and that of survivors. Notably, this remarkable difference was found at birth before the start of TH and was confirmed at the end of therapy, at 72 hours of life, as showed in *Figure 5*. Pathway analysis revealed the most affected metabolic pathways by perinatal asphyxia, as reported in *Figures 6* and 7. Among the 43, 31, 45, 43, and 40 pathways recognized at birth, 48, 72 h, 1 week, and 1 month of life, respectively, we reported the ten most important metabolic pathways for each time point. The pathways ranking is based on indexes described above: total value, hits value, raw P value, Holm P value, and impact value. During TH (samples collected at 48 and 72 hours, T1 and T2) the most impacting pathways on both molecular phenotypes were: phenylalanine metabolism, fructose and mannose metabolism, pyrimidine metabolism, glycolysis or gluconeogenesis, starch and sucrose metabolism, pentose phosphate pathway. After 1 week, molecular phenotype shared four pathways with that

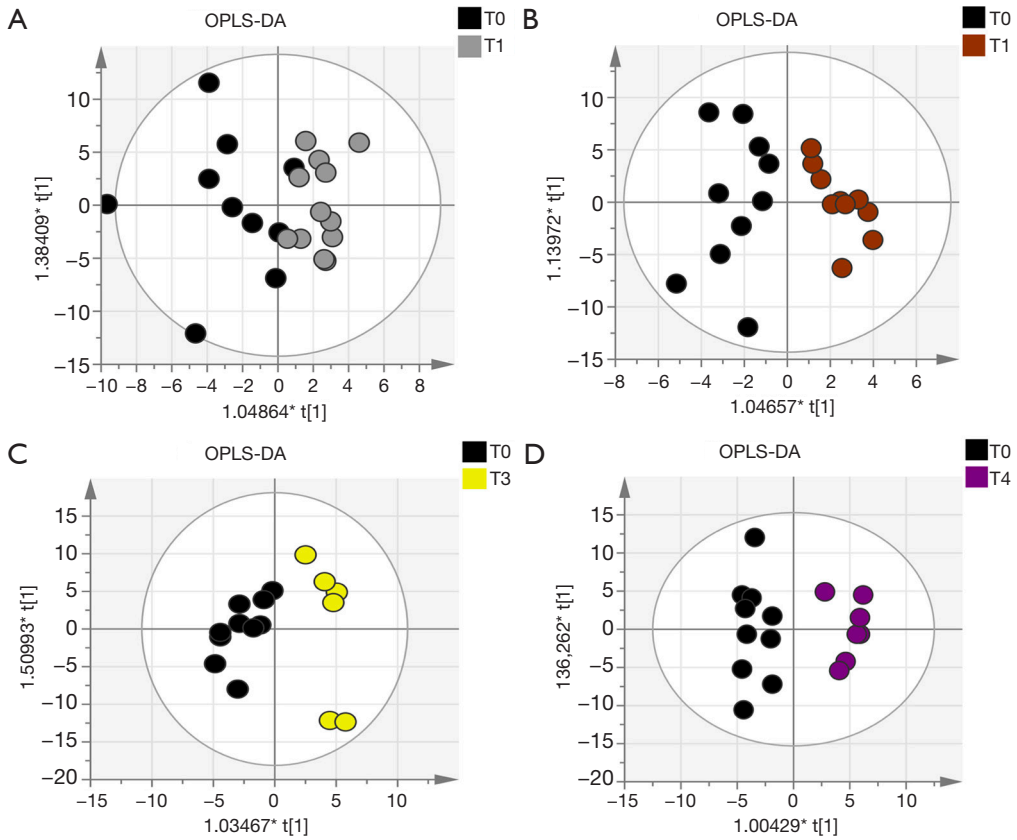

Figure 3 OPLS-DA of urine metabolic profile in perinatal asphyxia. Scores plot of the comparison of urine samples at birth before starting TH (T0, black dots) with: urine samples after 24 hours from birth, during TH (T1, gray dots, A); urine samples after 72 hours from birth, at the end of TH (T2, brown dots, B); urine samples after 1 week from birth (T3, yellow dots, C); urine samples after one month from birth (T4, purple dots, D). The X axes is the weighted score component t[1] whereas the Y axes is the orthogonal weighted score component t[1]. OPLS-DA, orthogonal partial least squares-discriminant analysis; TH, therapeutic hypothermia.

at birth: tyrosine metabolism, phenylalanine, tyrosine and tryptophan biosynthesis, ubiquinone and other terpenoid-quinone biosynthesis, nitrogen metabolism. Finally, at 1 month of life we found a consistent shift of the metabolic phenotype: among the first ten pathways, eight were not included previously.

Discussion

Perinatal asphyxia causes an imbalance in homeostasis of biological systems consisting of perturbation in gene expression and, in turn, in cellular activity. Metabolites represent the molecular endpoint or phenotype of the interplay between environment and gene expression and thus metabolomics offers a holist approach for the early and accurate evaluation of changes in dynamics of biological systems. Our results clearly suggest a dynamic change over time in urine metabolome of babies with perinatal asphyxia treated with hypothermia. In this study urine metabolome at birth, before the start of TH, was considered as landmark and no control group was selected and used as reference against which to compare results found in babies with perinatal asphyxia. In fact, it is reasonable to assume that in a NICU no baby can be considered "healthy"; moreover, hypoxia, ischemia and anoxia are commonly associated with several neonatal pathological conditions requiring intensive care. Accordingly, there is a high likelihood to include babies with asphyxia within a hypothetic "control group". Finally, information originating from the comparison of urine metabolome over time in babies with perinatal asphyxia is clinically more relevant and useful rather than the simple comparison with a theoretical control group.

T1 *vs*. T0		T2 *vs*. T0		T3 *vs*. T0		T4 *vs*. T0	
Increased	Decreased	Increased	Decreased	Increased	Decreased	Increased	Decreased
Lactose	Lactic acid	Lactose	Lactic acid	Lactose	Lactic acid		Lactic acid
	Taurine	Citric acid	Taurine	Citric acid	Taurine	Citric acid	Taurine
	Lysine	Galactose	Lysine	Galactose	Lysine	Galactose	Lysine
	Mannitol	Creatinine	Mannitol	Creatinine	Mannitol		Mannitol
	Oxalic acid	4-Hydroxyproline		4-Hydroxyproline	Oxalic acid		Oxalic acid
	Fructose		Fructose				Fructose
	N-Acetyl-glucosamine		N-Acetyl-glucosamine	Galactitol		Galactitol	N-Acetyl-glucosamine
	Kynurenic acid		Kynurenic acid				Kynurenic acid
	Sedoheptulose		Sedoheptulose				Sedoheptulose
	Ethanolamine				Ethanolamine		Ethanolamine
	Sucrose		Sucrose				Sucrose
	5-(Acetylamino)-3,5-dideoxy-D-glycero-galacto-2-nonulosonic acid		5-(Acetylamino)-3,5-dideoxy-D-glycero-galacto-2- nonulosonic acid				5-(Acetylamino)-3,5-dideoxy-D-glycero-galacto-2-nonulosonic acid
	Scylloinositol				Scylloinositol		Scylloinositol
	U1605				U1605		U1605
			U1455		U1455		U1455
	Monosacch. E		Monosacch. E				Monosacch. E
U1710		U1710			U1710		U1710

Figure 4 Most relevant changes in metabolites concentration over time in perinatal asphyxia. Urine metabolome at birth has been assumed as reference. T0, birth; T1, 48 hours; T2, 72 hours; T3, 1 week; T4, 1 month. Unknown metabolites are listed as: U1455, U1605, U1710 and Monosacch. E.

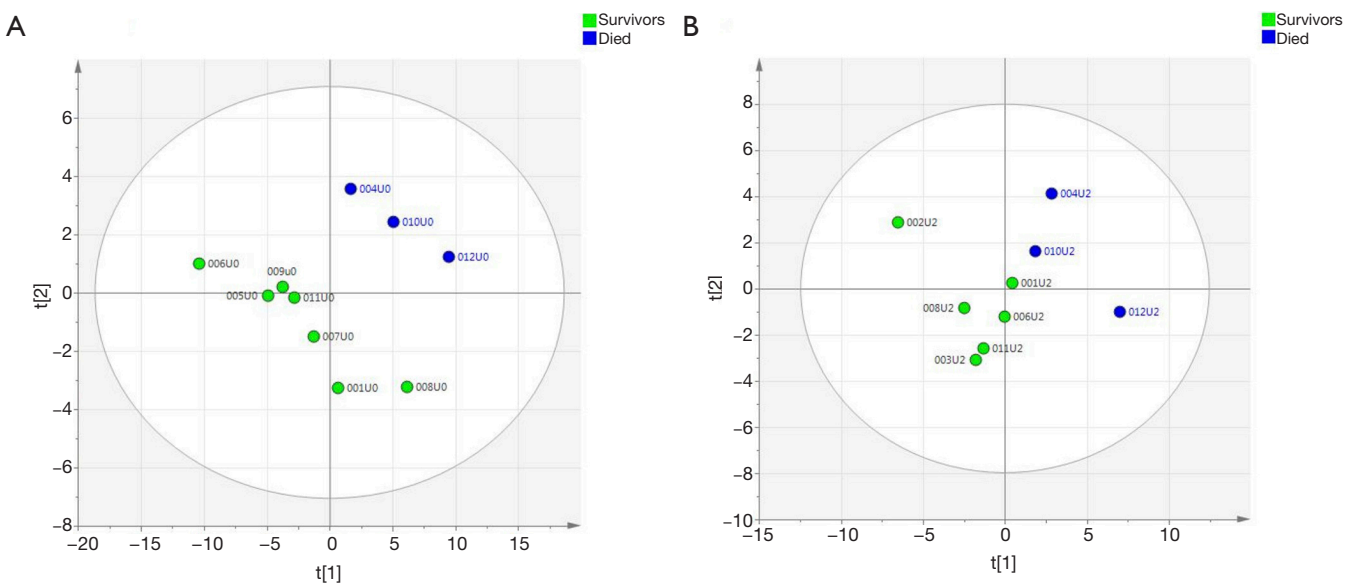

Figure 5 PLS-DA of urine metabolome at birth, before starting TH (A) and after 72 hours, at the end of therapy (B). In this plot, PLS-DA enables class separation (discrimination) analysis between survivors and died newborns. PLS-DA, partial least squares-discriminant analysis; TH, therapeutic hypothermia.

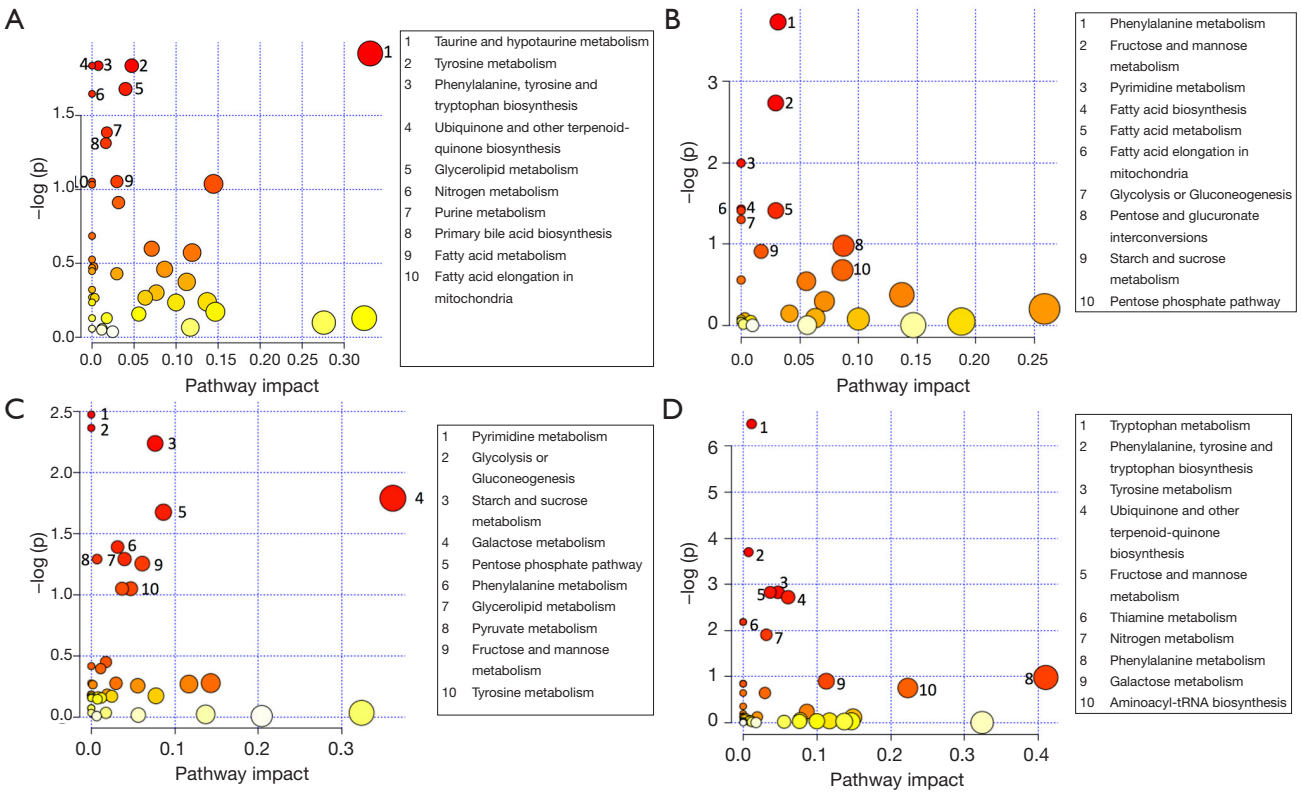

Figure 6 Metabolic pathway analysis at birth (A), after 24 hours from birth (B), after 72 hours (C), and after 1 week of life (D). Metabolic pathways are represented as circles according to their scores from enrichment (vertical axis) and topology analyses (pathway impact, horizontal axis). Darker circle colors indicate more significant changes of metabolites in the corresponding pathway. The size of the circle corresponds to the pathway impact score and is correlated with the centrality of the involved metabolites. A list of ranked pathways 1–10 based on their relevance to the given traits is reported on the left of each panel; corresponding numbers have been associated with symbols in the plots.

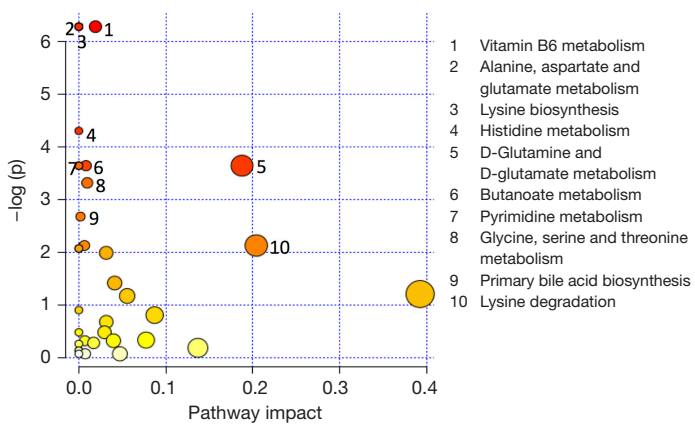

Figure 7 Metabolic pathway analysis after 1 month of life. Metabolic pathways are represented as circles according to their scores from enrichment (vertical axis) and topology analyses (pathway impact, horizontal axis). Darker circle colors indicate more significant changes of metabolites in the corresponding pathway. The size of the circle corresponds to the pathway impact score and is correlated with the centrality of the involved metabolites. A list of ranked pathways 1–10 based on their relevance to the given traits is reported on the left; corresponding numbers have been associated with symbols in the plot.

Several discriminant metabolites have been found persistently decreasing (lactic acid, taurine, lysine and mannitol) or increasing (citric acid, lactose and galactose) over time (*Figure 4*). The decrement of lactic acid over time from T1 to T4 in our population reflects the progressive recovery of aerobic metabolism. Notably, lactic acid was found significantly increased in the three dead babies, both in T0 and T2 (AUC 0.86 and 0.62, respectively). The role of lactic acid in the developing brain is that of an exchangeable substrate between astrocytes, the more abundant neuroglial cell type, and neurons; it is both a precursor of lipids and energy source for neurons. During hypoxia-anoxia, astrocytes consistently increase the lactic acid production rate by the activation of the anaerobic glycolysis pathway, with a progressive accumulation of this metabolite and, in turn, acidosis. The latter exerts a negative impact on astrocyte metabolism, leading to serious and irreversible astrocytes damage and cytolysis (41). The progressive loss in astrocytes number originates a redox imbalance caused by a massive generation of ROS and ultimately an additional damage to neurons, previously injured by the loss of energy source deriving from astrocytes. Our results confirm previous reports on the role of lactic acid as biomarker of poor outcome in perinatal hypoxia and HIE (42). Similarly to lactic acid, taurine (2-aminoethanesulfonic acid) decreased over time from T1 to T4 and was found increased in T2 in the group of dead babies (AUC =0.86). Taurine is synthesized from methionine and cysteine in the presence of vitamin B6. This metabolite is involved in the maintenance of intracellular sodium and calcium homeostasis and in the balance of neurotransmitters. In addition, taurine and its analogues exert anti-neurotoxic and anti-inflammatory effects (43). Being an intracellular metabolite, alterations in plasma membrane permeability and cytolysis give rise to the accumulation of extracellular taurine and therefore it may be considered a biomarker of cellular injury and death. As a consequence, the decrease over time in urinary taurine concentration can be explained by the progressive recovery of injured tissues and organs. Conversely, the high taurine urinary level in the group of dead babies may be considered an index of cell necrosis and death due to hypoxia. In a previous metabolomics study on babies with bronchopulmonary dysplasia (BPD) performed by proton nuclear magnetic resonance (^{1}H NMR), taurine showed a closely comparable behavior to that found in this study, confirming the key role of this metabolite in predicting clinical outcome (44). The trend over time of lysine is similar to that of lactic acid and taurine. Lysine is an essential amino acid mainly involved as a precursor in protein biosynthesis; in addition, lysine is a precursor in the biosynthesis of free carnitine and its esterified form acylcarnitine, two key metabolites for β-oxidation. In hypoxia-ischemia, the decrease of fatty acid oxidation causes an increase in carnitines concentrations (45). At birth we found very high levels of urinary lysine probably correlated with the increasing need of energy source by cells during hypoxia. Indeed, lysine can be used as an alternative fuel for cells, partially replacing the unavailability of aerobic metabolism (46). Subsequently, lysine decreased from T1 to T4 as a result of its consumption as a precursor of carnitine. It is reasonable to assume that the progressive decrease of mannitol over time together with its accumulation in the urine of dead babies at T2 (AUC =0.86) may be due to the presence of this metabolic inert substrate within pharmaceutical products as excipient (47). Mannitol is a carbon non-cyclic sugar alcohol and an isomer of sorbitol and can be used in clinical practice to preserve central nervous system. Our findings suggest that the decrease of mannitol over time is proportional to the reduction in drugs administration due to the amelioration of clinical conditions especially after TH; conversely, the high level observed in dead babies at 72 h may originate from the intensification of therapy in critical clinical conditions. Since persistent brain hypoxia and ischemia lead to brain hyperosmolality (48), the simultaneous increases of mannitol exacerbate the process (49). Ultimately, we cannot rule out the presence of gut dysbiosis in these babies; in particular Clostridium sp. HGF2, Streptococcus sp. M143, Streptococcus sp. M334 were found to be significantly associated with mannitol (50). On the other hand, the dysbiosis-induced hyperpermeability of the gut mucosa contributes to the increase of urine mannitol excretion (51). Citric acid was found persistently increasing from T1 to T4 when compared with T0. Citric acid is an intermediate in the TCA cycle. TCA cycle is the central metabolic hub of the cell, being the gateway to the aerobic metabolism of any molecule that can be transformed into an acetyl group or dicarboxylic acid. In addition, TCA cycle is a source of precursors for the building blocks of amino acids, nucleotide bases, cholesterol, and porphyrin. The increase of citric acid over time can be correlated with the progressive re-activation of oxygen-dependent ATP production pathways, namely the TCA cycle. This is confirmed by the finding of citric acid as a discriminant metabolite in survivors at 72 h (AUC =0.81). Interestingly, in survivors we found high levels of 2-ketoglutaric acid, an

intermediate of TCA cycle, both at birth (T0, AUC =0.86) and after 72 h (T2, AUC =0.81), strongly supporting the assumption that in these babies the aerobic pathways have been re-activated and its concomitant absence in dead babies. The trend of changes in carbohydrates urine level over time is characterized by the decrement of fructose at T1 and T2 together with the simultaneous increase of lactose and galactose from T1 to T4 and that of galactitol, the reduction product of galactose, at T3 and T4 (*Figure 4*). Fructose is metabolized in the liver, primarily to glycogen; the accumulation of fructose at birth and the subsequent decrease are consistent with the recovery of liver function over time. Lactose, a disaccharide of D-glucose and D-galactose, is present in milk and is the principal dietary source of galactose. Lactose is the primary carbohydrate source for developing mammals and in humans it constitutes 40% of the energy consumed during the nursing period. The progressive increase of lactose, galactose, and galactitol originates from feeding; in survivors, galactitol was found increased both at birth (AUC =0.81) and after 72 h (AUC =0.81), while galactose was increased at birth (AUC =0.81). 4-Hydroxyproline was found increased at T2 and T3. L-Proline, a non-essential amino acid synthesized from glutamic acid, is an essential component of collagen. The enzymatic hydroxylation of proline by prolylhydroxylase (PHD) forms hydroxyproline. In hypoxia, hydroxylation of proline is involved in targeting hypoxia-inducible factor alpha subunit (HIF-1α) by proteolysis (52). HIFs are transcription factors responding to changes in available oxygen within the cellular environment. The increase over time of hydroxyproline may be due to the positive response of the organism to the hypoxic condition; conversely, the high level of proline in dead babies at birth (AUC =0.76) may be considered a negative predictive factor of unfavorable outcome for the unavailability of proline hydroxylation and, in turn, HIF-1α synthesis. Degradation of 4-hydroxyproline results in the formation of glyoxylate; glyoxylate synthesis has clinical significance, as it is the only known precursor of oxalate. Glyoxylate derived from hydroxyprolin catabolism is normally metabolized by alanine: glyoxylate aminotransferase (AGT) and glyoxylate reductase (GR); GR plays a significant role in metabolizing the glyoxylate derived from hydroxyprolin breakdown and limiting its conversion to oxalate (53). However, the progressive decrease over time of oxalic acid may be due to the utilization of this metabolite for the synthesis of uracil and orotic acid (54) that in turn is involved in the cellular replication occurring during tissues and organs recovery after hypoxia.

Pathway analysis aimed to identify the most involved metabolism for each time point. Metabolic pathways are groups of metabolites that are related to the same biological process, and that are directly or indirectly connected by one or multiple enzymatic reactions. All the characterizing metabolites were identified and quantified by GC-MS and were used to discover the hub and spoke within each time point. At birth (*Figure 6A*), the most relevant pathways were the taurine and hypotaurine metabolism, tyrosine, and ubiquinone. As detailed above, taurine is an intracellular amino acid involved in the maintenance of homeostasis in terms of osmolarity and promotes the balance of neurotransmitters (55). Experimental *in vitro* studies on human neuroblastoma cells demonstrated that taurine exerts a robust protection effect against hypoxia and oxygen/glucose deprivation. Tyrosine is a non-essential amino acid synthesized in mammals from (L)-phenylalanine by phenylalanine hydroxylase. Tyrosine is a precursor of neurotransmitters: via tyrosine hydroxylase, dopamine can be further oxidized to L-norepinephrine that in turn is converted in L-epinephrine. Chronic hypoxia/ischemia reduces the activity of the enzymes causing neuronal deficiency (56). Ubiquinone is a lipid-soluble molecule located in the hydrophobic core of the mitochondrial membrane. Ubiquinone accepts the electrons both from complex I and complex II and then delivers electrons to complex III (57). In hypoxic conditions, ubiquinone is implicated in the production of ROS even if the role of mitochondrial ROS in the regulation of HIF-1 under hypoxia is still controversial (58). The remaining relevant metabolisms highlighted by the pathway analysis at birth are closely correlated with the absolute need of fuel for cellular homeostasis, namely glycerolipid, purine, and fatty acids metabolisms. At 48 h (*Figure 6B*), mitochondrial dysfunction and depolarization of neuronal cell membranes take place, leading to the production of ROS, whereby hypothermia appears to blunt this response via attenuation of oxidative stress. Pathway analysis at 48 hours reveals an activation of phenylalanine metabolism that may be related with neurotransmission; moreover, all the remaining metabolisms are implied in the generation of energetic substrates either via glycolysis or gluconeogenesis, or via fatty acid. At the end of the TH (*Figure 6C*), the pyrimidine biosynthesis is the most relevant pathway, being of importance for cell proliferation and for TCA cycle intermediates. Out of ten metabolisms listed as most important in the pathway analysis, eight aim

to provide energy to the organism after a period of lactic acid overproduction characterized by the depletion of ATP for maintaining cell membrane integrity and function. Tyrosine metabolism has been previously discussed (48 h). The same hubs are present at 1 week (*Figure 6D*) and at 1 month (*Figure 7*) suggesting a metabolic evolution towards the recovery by the activation of energetic pathways such as the TCA cycle.

Conclusions

Our study is affected by several limitations: the small number of newborns, the incomplete set of urine samples over time, and the lack of any investigation on gut microbiota composition over time. The latter seems to be the most important issue for elucidating the origin of a number of discriminant metabolites found in our study. However, we have extracted a plethora of data by comparing the urine metabolome at birth with those observed at each time point collection. In particular, we can assume that taurine may be considered a candidate biomarker for assessing and monitoring cellular injuries and death during a hypoxic-anoxic insult. Further investigations including a larger number of newborns are required for validating the assumption on taurine. Ultimately, it seems of great interest to discover in the near future the unknown metabolite U1710 in order to explain its controversial behavior over time.

Acknowledgments

Francesco Palmas gratefully acknowledges Sardinia Regional Government for the financial support of his PhD scholarship (P.O.R. Sardegna F.S.E. Operational Programme of the Autonomous Region of Sardinia, European Social Fund 2007–2013—Axis IV Human Resources, Objective l.3, Line of Activity l.3.1.). Authors thank Head Nurse Giuliana Cavallero and NICU Nurse Staff of Cuneo for their invaluable support.

Footnote

Conflicts of Interest: The authors have no conflicts of interest to declare.

Ethical Statement: The study was approved by the institutional ethics board of Cagliari (No. CA-206-18/03/2013) and written informed consent was obtained from all patients.

References

1. Sunshine P. Perinatal asphyxia: an overview. In: Stevenson DK, Benitz WE, Sunshine P. editors. Fetal and neonatal brain injury: mechanisms, management and the risks of practice. Third edition. Cambridge (UK): Cambridge University Press, 2003:3-28.
2. Committee on Obstetric Practice, American College of Obstetricians and Gynecologists. ACOG Committee Opinion. Number 326, December 2005. Inappropriate use of the terms fetal distress and birth asphyxia. Obstet Gynecol 2005;106:1469-70.
3. Ahearne CE, Boylan GB, Murray DM. Short and long term prognosis in perinatal asphyxia: An update. World J Clin Pediatr 2016;5:67-74.
4. Laptook AR. Birth Asphyxia and Hypoxic-Ischemic Brain Injury in the Preterm Infant. Clin Perinatol 2016;43:529-45.
5. Shah P, Riphagen S, Beyene J, et al. Multiorgan dysfunction in infants with post-asphyxial hypoxic-ischaemic encephalopathy. Arch Dis Child Fetal Neonatal Ed 2004;89:F152-5.
6. Herrera-Marschitz M, Neira-Pena T, Rojas-Mancilla E, et al. Perinatal asphyxia: CNS development and deficits with delayed onset. Front Neurosci 2014;8:47.
7. Wassink G, Gunn ER, Drury PP, et al. The mechanisms and treatment of asphyxial encephalopathy. Front Neurosci 2014;8:40.
8. Antonucci A, Porcella A, Pilloni MD. Perinatal asphyxia in the term newborn. J Ped Neonat Individ Med 2014;3:e030269.
9. Liang D, Bhatta S, Gerzanich V, et al. Cytotoxic edema: mechanisms of pathological cell swelling. Neurosurg Focus 2007;22:E2.
10. Watson JA, Watson CJ, McCann A, et al. Epigenetics, the epicenter of the hypoxic response. Epigenetics 2010;5:293-6.
11. Mimura I, Tanaka T, Wada Y, et al. Pathophysiological response to hypoxia - from the molecular mechanisms of malady to drug discovery: epigenetic regulation of the hypoxic response via hypoxia-inducible factor and histone modifying enzymes. J Pharmacol Sci 2011;115:453-8.
12. Smith TF, Schmidt-Kastner R, McGeary JE, et al. Pre- and Perinatal Ischemia-Hypoxia, the Ischemia-Hypoxia Response Pathway, and ADHD Risk. Behav Genet 2016;46:467-77.
13. Azzopardi DV, Strohm B, Edwards AD, et al. Moderate hypothermia to treat perinatal asphyxial encephalopathy.

N Engl J Med 2009;361:1349-58.
14. Azzopardi D, Strohm B, Marlow N, et al. Effects of hypothermia for perinatal asphyxia on childhood outcomes. N Engl J Med 2014;371:140-9.
15. Laptook AR, Corbett RJ, Sterett R, et al. Quantitative relationship between brain temperature and energy utilization rate measured in vivo using 31P and 1H magnetic resonance spectroscopy. Pediatr Res 1995;38:919-25.
16. Thoresen M. Cooling after perinatal asphyxia. Semin Fetal Neonatal Med 2015;20:65.
17. Noto A, Fanos V, Dessì A. Metabolomics in Newborns. Adv Clin Chem 2016;74:35-61.
18. Koen N, Du Preez I, Loots du T. Metabolomics and Personalized Medicine. Adv Protein Chem Struct Biol 2016;102:53-78.
19. Solberg R, Enot D, Deigner HP, et al. Metabolomic analyses of plasma reveals new insights into asphyxia and resuscitation in pigs. PLoS One 2010;5:e9606.
20. Fanos V, Noto A, Xanthos T, et al. Metabolomics network characterization of resuscitation after normocapnic hypoxia in a newborn piglet model supports the hypothesis that room air is better. Biomed Res Int 2014;2014:731620.
21. Sachse D, Solevåg AL, Berg JP, et al. The Role of Plasma and Urine Metabolomics in Identifying New Biomarkers in Severe Newborn Asphyxia: A Study of Asphyxiated Newborn Pigs following Cardiopulmonary Resuscitation. PLoS One 2016;11:e0161123.
22. Chu CY, Xiao X, Zhou XG, et al. Metabolomic and bioinformatic analyses in asphyxiated neonates. Clin Biochem 2006;39:203-9.
23. Walsh BH, Broadhurst DI, Mandal R, et al. The metabolomic profile of umbilical cord blood in neonatal hypoxic ischaemic encephalopathy. PLoS One 2012;7:e50520.
24. Reinke SN, Walsh BH, Boylan GB, et al. 1H NMR derived metabolomic profile of neonatal asphyxia in umbilical cord serum: implications for hypoxic ischemic encephalopathy. J Proteome Res. 2013;12:4230-9.
25. Lou BS, Wu PS, Liu Y, et al. Effects of acute systematic hypoxia on human urinary metabolites using LC-MS-based metabolomics. High Alt Med Biol 2014;15:192-202.
26. Denihan NM, Boylan GB, Murray DM. Metabolomic profiling in perinatal asphyxia: a promising new field. Biomed Res Int 2015;2015:254076.
27. Longini M, Giglio S, Perrone S, et al. Proton nuclear magnetic resonance spectroscopy of urine samples in preterm asphyctic newborn: a metabolomic approach. Clin Chim Acta 2015;444:250-6.
28. Fattuoni C, Palmas F, Noto A, et al. Perinatal asphyxia: a review from a metabolomics perspective. Molecules 2015;20:7000-16.
29. Sarnat HB, Sarnat MS. Neonatal encephalopathy following fetal distress. A clinical and electroencephalographic study. Arch Neurol 1976;33:696-705.
30. Bayley N. Bayley scales of infant and toddler development: Bayley-III. Harcourt Assessment, San Antonio, TX, USA, 2006. Available online: http://www.pearsonclinical.com/childhood/products/100000123/bayley-scales-of-infant-and-toddler-development-third-edition-bayley-iii.html
31. Oberacher H, Whitley G, Berger B. Evaluation of the sensitivity of the 'Wiley registry of tandem mass spectral data, MSforID' with MS/MS data of the 'NIST/NIH/EPA mass spectral library'. J Mass Spectrom 2013;48:487-96.
32. Kopka J, Schauer N, Krueger S, et al. GMD@CSB. DB: the Golm Metabolome Database. Bioinformatics 2005;21:1635-8.
33. Bro R, Smilde AK. Principal component analysis. Anal Methods 2014;6:2812-31.
34. Robotti E, Marengo E. Chemometric Multivariate Tools for Candidate Biomarker Identification: LDA, PLS-DA, SIMCA, Ranking-PCA. Methods Mol Biol 2016;1384:237-67.
35. Barupal DK, Haldiya PK, Wohlgemuth G, et al. MetaMapp: mapping and visualizing metabolomic data by integrating information from biochemical pathways and chemical and mass spectral similarity. BMC Bioinformatics 2012;13:99.
36. Triba MN, Le Moyec L, Amathieu R, et al. PLS/OPLS models in metabolomics: the impact of permutation of dataset rows on the K-fold cross-validation quality parameters. Mol Biosyst 2015;11:13-9.
37. Tsugawa H, Tsujimoto Y, Arita M, et al. GC/MS based metabolomics: development of a data mining system for metabolite identification by using soft independent modeling of class analogy (SIMCA). BMC Bioinformatics 2011;12:131.
38. Akarachantachote N, Chadcham S, Saithanu K. Cutoff Threshold of Variable Importance in Projection for Variable Selection. Int J Pure Appl Mathematics 2014;94:307-22.
39. Xia J, Sinelnikov IV, Han B, et al. MetaboAnalyst 3.0--making metabolomics more meaningful. Nucleic Acids Res 2015;43:W251-7.
40. Grapov D, Wanichthanarak K, Fiehn O. MetaMapR: pathway independent metabolomic network analysis

incorporating unknowns. Bioinformatics 2015;31:2757-60.
41. Romero J, Muñiz J, Logica Tornatore T, et al. Dual role of astrocytes in perinatal asphyxia injury and neuroprotection. Neurosci Lett 2014;565:42-6.
42. Ide Bergamaschi N, Clarke P. Is delayed normalization of plasma lactate in cooled babies with hypoxic-ischaemic encephalopathy associated with a poor outcome? J Pediatr Neonat Individual Med 2015;4:36-7.
43. Marcinkiewicz J, Kontny E. Taurine and inflammatory diseases. Amino Acids 2014;46:7-20.
44. Fanos V, Pintus MC, Lussu M, et al. Urinary metabolomics of bronchopulmonary dysplasia (BPD): preliminary data at birth suggest it is a congenital disease. J Matern Fetal Neonatal Med 2014;27 Suppl 2:39-45.
45. Ezgü FS, Atalay Y, Hasanoğlu A, et al. Serum carnitine levels in newborns with perinatal asphyxia and relation to neurologic prognosis. Nutr Neurosci 2004;7:351-6.
46. Jones LL, McDonald DA, Borum PR. Acylcarnitines: role in brain. Prog Lipid Res 2010;49:61-75.
47. Amstrong NA. Mannitol. In: Rowe RC, Sheskey PJ, Quinn ME. editors. Handbook of Pharmaceutical Excipients. 6th edition. London (UK): Pharmaceutical Press and American Pharmacists Association, 2009:424-8.
48. Hatashita S, Hoff JT, Salamat SM. Ischemic brain edema and the osmotic gradient between blood and brain. J Cereb Blood Flow Metab 1988;8:552-9.
49. Polderman KH, van de Kraats G, Dixon JM, et al. Increases in spinal fluid osmolarity induced by mannitol. Crit Care Med 2003;31:584-90.
50. Feng Q, Liu Z, Zhong S, et al. Integrated metabolomics and metagenomics analysis of plasma and urine identified microbial metabolites associated with coronary heart disease. Sci Rep 2016;6:22525.
51. Nathavitharana KA, Lloyd DR, Raafat F, et al. Urinary mannitol: lactulose excretion ratios and jejunal mucosal structure. Arch Dis Child 1988;63:1054-9.
52. Jaakkola P, Mole DR, Tian YM, et al. Targeting of HIF-alpha to the von Hippel-Lindau ubiquitylation complex by O2-regulated prolyl hydroxylation. Science 2001;292:468-72.
53. Jiang J, Johnson LC, Knight J, et al. Metabolism of [13C5] hydroxyproline in vitro and in vivo: implications for primary hyperoxaluria. Am J Physiol Gastrointest Liver Physiol 2012;302:G637-43.
54. Robertson DS. The function of oxalic acid in the human metabolism. Clin Chem Lab Med 2011;49:1405-12.
55. Guizouarn H, Motais R, Garcia-Romeu F, et al. Cell volume regulation: the role of taurine loss in maintaining membrane potential and cell pH. J Physiol 2000;523 Pt 1:147-54.
56. White LD, Lawson EE. Effects of chronic prenatal hypoxia on tyrosine hydroxylase and phenylethanolamine N-methyltransferase messenger RNA and protein levels in medulla oblongata of postnatal rat. Pediatr Res 1997;42:455-62.
57. Klimova T, Chandel NS. Mitochondrial complex III regulates hypoxic activation of HIF. Cell Death Differ 2008;15:660-6.
58. Solaini G, Baracca A, Lenaz G, et al. Hypoxia and mitochondrial oxidative metabolism. Biochim Biophys Acta 2010;1797:1171-7.

Cite this article as: Noto A, Pomero G, Mussap M, Barberini L, Fattuoni C, Palmas F, Dalmazzo C, Delogu A, Dessì A, Fanos V, Gancia P. Urinary gas chromatography mass spectrometry metabolomics in asphyxiated newborns undergoing hypothermia: from the birth to the first month of life. Ann Transl Med 2016;4(21):417. doi: 10.21037/atm.2016.11.27

